Research Article

Full-Spectrum *Cannabis* Extract Microdepots Support Controlled Release of Multiple Phytocannabinoids for Extended Therapeutic Effect

Almog Uziel, Anat Gelfand, Keren Amsalem, Paula Berman, Gil M. Lewitus, David Meiri,*
and Dan Y. Lewitus*

Cite This: https://dx.doi.org/10.1021/acsami.0c04435

Read Online

ACCESS | Metrics & More | Article Recommendations | SI Supporting Information

ABSTRACT: The therapeutic effect of the *Cannabis* plant largely depends on the presence and specific ratio of a spectrum of phytocannabinoids. Although prescription of medicinal *Cannabis* for various conditions constantly grows, its consumption is mostly limited to oral or respiratory pathways, impeding its duration of action, bioavailability, and efficacy. Herein, a long-acting formulation in the form of melt-printed polymeric microdepots for full-spectrum cannabidiol (CBD)-rich extract administration is described. When injected subcutaneously in mice, the microdepots facilitate sustained release of the encapsulated extract over a two-week period. The prolonged delivery results in elevated serum levels of multiple, major and minor, phytocannabinoids for over 14 days, compared to *Cannabis* extract injection. A direct analysis of the microdepots retrieved from the injection site gives rise to an empirical model for the release kinetics of the phytocannabinoids as a function of their physical traits. As a proof of concept, we compare the long-term efficacy of a single administration of the microdepots to a single administration of *Cannabis* extract in a pentylenetetrazol-induced convulsion model. One week following administration, the microdepots reduce the incidence of tonic-clonic seizures by 40%, increase the survival rate by 50%, and the latency to first tonic-clonic seizures by 170%. These results suggest that a long-term full-spectrum *Cannabis* delivery system may provide new form of *Cannabis* administration and treatments.
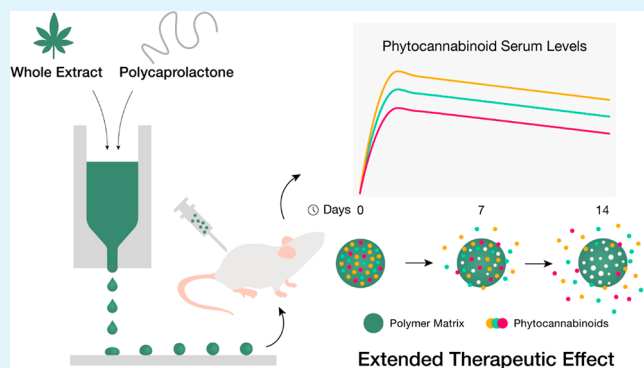
1. INTRODUCTION

A central principle underlying the use of whole-plant medicines is that herbs are inherently polypharmaceutical. The potential synergy between the vast number of active ingredients contained in herbs has garnered attention in the phytomedicine field in recent years. Of all the plant species with therapeutic properties, *Cannabis* is one of the most versatile in terms of its phytochemistry.[1−3] More than 500 natural compounds belonging to a broad range of chemical classes have been identified or isolated from *Cannabis*.[4,5] The most abundant are the phytocannabinoids (plant-derived cannabinoids), a family of terpenophenolic compounds uniquely produced by the plant as secondary metabolites.[6,7] Gill et al.,[8] showed that the activity of Δ^9-*trans*-tetrahydrocannabinol (Δ^9-THC), the primary active ingredient of *Cannabis*, is influenced by other compounds present in the plant, promoting the notion of phytochemical synergy in *Cannabis* pharmacology.[9−12] Gallily et al.,[13] reported that the bell-shaped dose–response of purified CBD, another major constituent of *Cannabis*, is partially alleviated by other phytocannabinoids or

noncannabinoids present in the plant. Recently, it was demonstrated that CBD-rich extracts of *Cannabis* have a superior therapeutic profile for treating refractory epilepsy compared to the isolated cannabinoid.[14] These results were supported by the finding that different high-CBD containing *Cannabis* strains produced different anticonvulsant properties in a pentylenetetrazol (PTZ) test in mice, despite having similar CBD content.[5] These differences may arise from pharmacokinetic and pharmacodynamic drug interactions, whose combined therapeutic effects are greater than the sum of their parts.[4,9,15,16]

In recent years, *Cannabis* use for medical purposes continues to evolve, as shown by the growing number of states now

A

permitting its administration for a variety of conditions, including chronic pain, cancer associated pain, chemotherapy-induced nausea and vomiting, spacticity associated with multiple scelerosis, Parkinson's disease, post-traumatic stress disorder, and intractable epilepsy.[12,17] Currently, the administration of whole-plant *Cannabis* is mainly through inhalation pathways, via vaporization or smoking, or by oral ingestion of edible products.[18,19] Such consumption sharply increases the therapeutic ingredient levels in the bloodstream and is followed by a short therapeutic action period, lasting no longer than several hours.[12,20,21] In addition, phytocannabinoids are lipophilic molecules with low aqueous solubility and susceptibility to degradation, limiting their oral bioavailability. Furthermore, phytocannabinoids absorption is highly dependent on various factors, such as their lipophilic nature, whether the patient had eaten recently, or inhalation conditions.[10,12,22] These limiting factors may be overcome via the development of novel dosage forms that are specifically designed to improve the therapeutic efficacy of active substances.[10,23]

Polymeric microspheres that are employed to encapsulate, protect, and deliver pharmaceuticals in a rate-controlled manner are potentially an attractive dosage form. In these systems, the polymer matrix acts as a carrier that modulates drug release kinetics, significantly extending its residence time and bioavailability, while reducing plasma levels fluctuations and administration frequency.[24,25] Several polymeric systems based on poly(lactic-*co*-glycolic acid) and polycaprolactone (PCL) have been developed in recent years for long-term delivery of CBD, Δ^9-THC and the cannabinoid derivative 1-naphthalenyl[4-(pentyloxy)-1-naphthalenyl]methanone (CB13). In vitro, these systems demonstrated sustained release over a two to three week period,[26−29] and inhibition of cancer cell proliferation.[27,28] In addition, the ability of the polymeric carriers to improve oral absorption[22] and extend the pain-relieving effect of CB13[30] has been shown in vivo. Moreover, the continuous release of CBD or Δ^9-THC reduced the growth of glioma xenografts in tumor-bearing mice,[31] and the incorporation of CBD-loaded microspheres in an osteoconductive scaffold improved bone healing.[32] However, the encapsulation and delivery of the whole *Cannabis* plant extract, critical for exploiting synergistic effects, using polymeric carriers has not been reported. In the present study, we aimed to develop polymer-based microdepots as a controlled-release *Cannabis* formulation. To this end, PCL microdepots loaded with whole-plant medicinal *Cannabis* extract were produced via melt printing and characterized in terms of physiochemical characteristics, encapsulation efficiency and release behavior in vitro and in vivo. Furthermore, the release of phytocannabinoids into the systemic circulation and its effect on PTZ-induced convulsions in a mouse model was compared to a bolus of pure *Cannabis* extract as a proof of concept for the therapeutic potential of the microdepots.

2. MATERIALS AND METHODS

2.1. Materials. PCL (Mw ∼ 14 000), carboxymethylcellulose (CMC), Tween 20, cremophor, phosphate buffered saline (PBS, pH 7.4), liquid chromatography−mass spectrometry (LC/MS) grade acetic acid, and high-performance liquid chromatography (HPLC) grade dichloromethane were purchased from Sigma-Aldrich (Rehovot, Israel). LC/MS grade acetonitrile, methanol, and water, and HPLC grade ethanol were obtained from Mercury Scientific and Industrial Products Ltd. (Rosh Haayin, Israel) or Bio-Lab Ltd. (Jerusalem, Israel). (−)-*trans*-Δ^9-tetrahydrocannabinolic acid (Δ^9-THCA), cannabidiolic acid (CBDA), cannabigerolic acid (CBGA),

cannabichromenic acid (CBCA), cannabinolic acid (CBNA), cannabidivarinic acid (CBDVA), Δ^9-THC, CBD, cannabigerol (CBG), cannabichromene (CBC), CBN, (−)-*trans*-Δ^9-tetrahydrocannabivarin (Δ^9-THCV), cannabidivarin (CBDV), cannabichromevarin (CBCV), Δ^9-THC-d3, CBD-d3, and CBN-d3 were purchased from Sigma-Aldrich (Rehovot, Israel). All the phytocannabinoid standards were of analytical grade (>98%).

2.2. *Cannabis* Extraction and Analysis. Air-dried medical *Cannabis* female flowers were ground to a fine powder using an electrical grinder, and heat-decarboxylated in an oven at 130 °C for 1 h. Approximately 30 g of the decarboxylated flowers were accurately weighed and extracted with 300 mL ethanol. Samples were sonicated in an ultrasonic bath for 30 min and then agitated in an orbital shaker at 25 °C for 15 min. Samples were filtered under pressure through Whatman No. 4 filter paper and the ethanol was evaporated at 38 °C under reduced pressure using a rotary evaporator (Laborata 4000; Heidolph Instruments GmbH & Co. KG; Germany). A sample of the extract was analyzed for phytocannabinoid composition using a Thermo Scientific ultrahigh-performance liquid chromatography (UHPLC) system coupled with a Q Exactive Focus Hybrid Quadrupole-Orbitrap MS (Thermo Scientific, Bremen, Germany). The chromatographic method and MS parameters are detailed in Phytocannabinoid Analysis Method 1 (see Methods in the Supporting Information). Identification and absolute quantification of phytocannabinoids was performed by external calibrations as described by Berman et al.[5]

2.3. Microdepot Preparation. Microdepots encapsulating whole-plant *Cannabis* extract were prepared via a melt printing technique.[33] Briefly, molten PCL was mixed with 30 wt % CBD-rich extract at 60 °C. Then, the mixture was jetted through a 100 μm flat nozzle onto nonwetting surfaces using a pneumatic jetting apparatus (P-Dot CT, Liquidyn [Nordson EFD], Oberhaching, Germany). A fluid temperature of 90 °C, fluid pressure of 0.1 bar, valve pressure of 4.9−5.1 bar, spring tightness of 0.6 turns and distance of ∼10 mm between the nozzle and the surface were applied to form discrete microspheres. The microdepots were left to cool to room temperature and stored at −4 °C until further use. The formation of the microdepots was captured using a digital high-speed camera (120 Phantom v12) equipped with a microscopic lens (Nikon 10 x CFI Plan Achromat), at a frame rate of 48 000−58 000 fps.

2.4. Microdepot Characterization. The particle size and size distribution of the microdepots were determined using a Malvern Mastersizer 3000 laser diffraction particle sizer (with a Hydro EV unit). The surface morphology of the microdepots was observed using a scanning electron microscopy. The microdepots were sputter-coated with Au−Pd alloy and then imaged using a JEOL JSM-IT200 SEM operated at an acceleration voltage of 20 kV. The appearance of the microdepots was imaged using a Dino-Lite Premier AM7013MZT digital hand-held microscope.

2.5. Phytocannabinoid Encapsulation Efficiency. *Cannabis* extract microdepots (approximately 3 mg) were dissolved in 200 μL of dichloromethane, then precipitated with 4 mL ethanol followed by vortex for 1 h. The suspension was filtered through 0.22 μm PTFE-filters to remove polymeric debris, and analyzed for phytocannabinoid concentration with a Thermo Scientific UHPLC system coupled with an ISQ EC Single Quadrupole MS (Thermo Scientific, Bremen, Germany) as described in Phytocannabinoid Analysis Method 2 (see Methods in the Supporting Information). Phytocannabinoid encapsulation efficiencies were determined by dividing the measured phytocannabinoid content by the theoretical value. Only phytocannabinoids constituting more than 0.5 wt % of the extract were reported.

2.6. Thermal Stability. To examine the long-term thermal stability of the *Cannabis* extract at the processing temperature, we kept the molten mixture at 90 °C and sampled at 1, 10, 20, and 30 h time points. The samples were prepared and analyzed by LC/MS as described in the former section to determine phytocannabinoids content.

2.7. In Vitro Release Study. In vitro release kinetics of phytocannabinoids from the polymeric microdepots was determined by incubation in PBS under sink conditions. Microdepots weighing

approximately 6 mg were suspended in 20 mL PBS (pH 7.4) containing 0.1% w/v Tween 20 at 37 °C under constant agitation. At predetermined time intervals, the release medium was withdrawn and replenished with fresh prewarmed medium. The obtained supernatant was freeze-dried, dissolved in 1 mL of ethanol, filtered, and then analyzed for phytocannabinoid content by LC/MS (see Phytocannabinoid Analysis Method 2 in Methods in the Supporting Information). SEM analyses were employed as previously described, to determine changes in microdepot sizes and surface morphologies during the dissolution test, and optical images were taken to follow their appearance.

2.8. In Vivo Release Study and Pharmacokinetics. The in vivo release characteristics of the microdepots were studied in mice. Animal studies were performed in compliance with the *Guide for the Care and Use of Laboratory Animals* established by the National Institutes of Health. All procedures and protocols were approved by the Technion Administrative Panel of Laboratory Animal Care (#:IL_050−05−2018). Adult male mice weighing 20−25 g (C57BL/6 J; The Jackson Laboratory) were randomly assigned to two groups and treated with either *Cannabis* extract microdepots or a *Cannabis* extract solution. Samples of *Cannabis* extract microdepots were suspended in 1 mL injection medium containing 1% w/w carboxymethylcellulose and 1% w/w Tween20 in saline.[34] The suspended microdepots were then administrated via subcutaneous injection through a 20g syringe into mice at a dose of 200 mg/kg extract under isoflurane anesthesia. As a control, *Cannabis* extract dissolved in 1:1:18 ethanol:cremophor:injection medium (25 mg/mL), was injected subcutaneously at an equivalent dose. Four mice from each group were sacrificed at 1, 2, 3, 7, and 14 days postadministration, and blood samples were collected via cardiac puncture. Blood samples were set aside for 30 min at room temperature and then centrifuged for 30 min at 4 °C. Serum was collected and stored at −80 °C until analysis. Area under curve (AUC) values were calculated directly from the serum concentration−time curve using the linear trapezoidal method, from the first day to the last time point.

Phytocannabinoid extraction from serum was performed as follows: 600 μL of the extraction solution (0.1% v/v acetic acid in a methanol:acetonitrile 1:1 mixture) spiked with 20 ng/mL deuterated internal standards (ISs) were added to 200 μL of serum samples. Samples were thoroughly vortexed and then centrifuged for 20 min at 4 °C for protein and cell precipitation. The supernatants were then transferred into 3 mL of 0.1% v/v acetic acid in water, and loaded onto Agela Cleanert C8 solid phase extraction (SPE) cartridges (500 mg of sorbent, 50 μm particle size). Phytocannabinoids were eluted from the columns using 2 mL of 0.1% v/v acetic acid in methanol, evaporated to dryness by speedvac, and reconstituted in 100 μL of ethanol. Phytocannabinoids in serum samples were analyzed using a Thermo Scientific UHPLC system coupled with a Q Exactive Focus Hybrid Quadrupole-Orbitrap MS (Thermo Scientific, Bremen, Germany).[5] The chromatographic and mass spectrometric parameters were the same as those described in Phytocannabinoid Analysis Method 1 (see Methods in the Supporting Information). For quantification of phytocannabinoids in serum samples, phytocannabinoid standards were prepared in ethanol to concentrations ranging from 0.2 to 2000 ng/mL for Δ^9-THCA, Δ^9-THC, CBDA, and CBD, and 0.125 to 500 ng/mL for all the other components. Standard calibration curves were then constructed by adding similar volumes of each concentration standard and a mixture of all deuterated ISs at a concentration of 30 ng/mL. The ratios of the unlabeled and labeled ions were plotted against the amounts of spiked standards, and the calibration curves were determined empirically according to a weighted least-squares linear regression method with a weighting factor of $1/X$.

At the same time points, the microdepots were collected from the injection site, washed with ddH$_2$O to remove cellular debris, and freeze-dried. Samples of dried microdepots (approximately 3 mg) were then dissolved in dichloromethane and prepared for LC/MS analysis as described in the Encapsulation Efficiency section to determine the remaining phytocannabinoid content. In addition, the

morphology and appearance of the microdepots after release were documented.

2.9. Microdepot Anticonvulsant Activity. The anticonvulsant activity assay was based on previous work.[5] One week following administration of *Cannabis* extract microdepots or *Cannabis* extract solution (as described above), mice (n = 10) were subcutaneously injected with PTZ by a treatment-blind experimenter at a dose of 80 mg/kg and then monitored for 30 min. The epileptic seizures were captured using a video recording system for epileptic seizures analysis in real-time (SeizureScan, Clever Sys., Inc., Virginia, USA), and the progress of seizure activity from normal behavior (P0) to behavior arrest (P1), to twitches (P2), to forelimb clonus (P3), to generalized clonic convulsions (P4), to tonic-clonic convulsions (P5) was recorded. The latency to first P5 convulsions, incidence of P5 convulsing animals and survival were analyzed. Following this monitoring, blood samples were collected from surviving mice via cardiac puncture to determine phytocannabinoid serum levels.

2.10. Statistical Analysis. In the microdepots characterization and release studies, data were determined as mean ± SD. In the study of microdepot anticonvulsant activity, the latency to first tonic-clonic seizures was determined as mean ± SEM. Significant differences in latency between experimental groups were determined using a paired student t test with p value <0.05. Percent of protection against development of tonic-clonic seizure and death subsequent to PTZ administration was compared using the χ^2 test with p value >0.05 for both seizure protection and mortality protection.

3. RESULTS

3.1. Formation and Characterization of *Cannabis*-Loaded Microdepots. The phytocannabinoid profile of the decarboxylated high-CBD *Cannabis* extract used in this study appears in Table 1. The extract contained more than 50 wt %

Table 1. Phytocannabinoid Profile of the Decarboxylated High-CBD *Cannabis* Extract, And Their Encapsulation Efficiencies (EEs) in PCL Microdepots Loaded with 30 wt % Extract

phytocannabinoid	content (wt %)	EE (%)
CBD	54.68	102.5 ± 0.6
CBDA	2.50	92.1 ± 1.2
Δ^9-THC	2.36	103.5 ± 2.4
CBG	2.35	90.0 ± 4.1
CBC	2.17	93.5 ± 2.1
CBDV	1.65	101.1 ± 3.7
CBDVA	0.42	
CBN	0.20	
Δ^9-THCV	0.17	
CBGA	0.09	

CBD and five other phytocannabinoids, CBDA, CBG, Δ^9-THC, CBC, and CBDV, having a weight percent above 0.5%. After mixing the liquid extract with the molten PCL, a solid mixture was obtained upon cooling, entrapping 30 wt % of the whole extract. A melt printing technique[33,35] was employed to produce polymeric microdepots. The deposition of the molten mixture on top of nonwetting surfaces using a pneumatic jetting apparatus operating at temperatures above the melting point of the polymeric system, yielded discrete, near-perfect spherical microparticles. Figure 1A shows a sequence of images captured using a high-speed camera emphasizing the spontaneous formation of an extract-loaded microsphere, upon interaction of the molten jet with the oleophobic substrate (the captured video can be seen in Video S1). The microspheres preserve their spherical shape during solid-
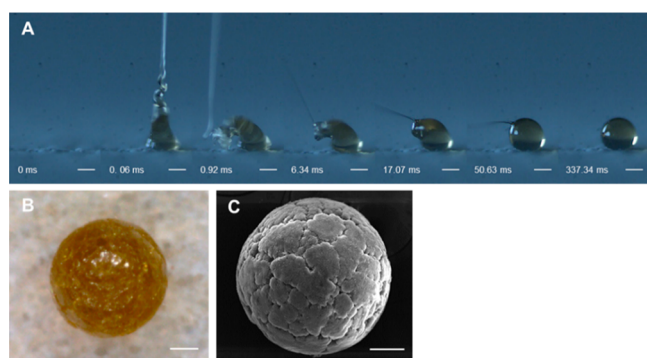
Figure 1. Formation of *Cannabis* extract microdepots. (A) Sequential images showing the evolution of a PCL microdepot loaded with 30 wt % *Cannabis* extract onto a nonwetting surface. (B) Optical and (C) SEM micrographs of a resulting microdepot. Scale bar: (A) 100 and (B, C) 50 μm.

ification and appear brown in color (Figure 1B). Scanning electron microscopy (SEM) images revealed round, uniform, and individualized microparticles, with a textured surface (Figure 1C), distinct from the smooth surface obtained for neat PCL microspheres printed from melt.[35] The particle size distribution was narrow and monodispersed, with a d_{50} of 257.80 $\pm$ 2.49 μm and a span value of 0.68 $\pm$ 0.05 μm, as measured using laser diffraction analysis (Figure S1).

Recent developments in the field of micro- or nanoparticles for controlled phytocannabinoid delivery involve only single constituents, such as CBD,[27,31,32] Δ^9-THC,[28,31] and CB13.[26,30,36] None have described the encapsulation of the full spectrum of *Cannabis* phytocannabinoids. Here, we were able to encapsulate all the phytocannabinoids present in the extract above 0.5 wt %, with encapsulation efficiencies of more than 90% (Table 1). This high encapsulation efficiency is possibly due to the closed environment of the melt processing and the exclusion of organic solvents.[33,37] However, one potential concern with melt processing techniques involves the exposure of active pharmaceutical ingredients to elevated temperatures.[38,39] Considering phytocannabinoid susceptibility to heat degradation,[40] the thermal stability of the phytocannabinoids in the polymeric matrix was studied during and postprocessing. Figure S2 shows that phytocannabinoid compositions remained nearly constant during microdepot printing and within the first 10 h. Afterward, a decrease in CBDA, CBD, and Δ^9-THC contents and an increase in cannabinol (CBN) content were detected, possibly due to decarboxylation of the acidic phytocannabinoids to their neutral forms and oxidation reactions.[15,41,42]

3.2. In Vitro Phytocannabinoids Release. Prior to the in vivo study, we evaluated the feasibility of the polymeric carrier to sustain phytocannabinoids release in vitro, under simulated physiological conditions. Figure 2A presents the in vitro release profiles, over 21 days, of the different phytocannabinoids in the extract-loaded microdepots. The microdepots showed a sustained release profile, in total releasing 70% of the entrapped predominant phytocannabinoid, CBD, and 52−64% CBDV, CBG, Δ^9-THC, and CBC with no initial burst release. CBDA, the acidic precursor of CBD, was released much faster than the other neutral phytocannabinoids, accounting for 70% cumulative release after 1 day, probably because of its higher aqueous solubility that increased the
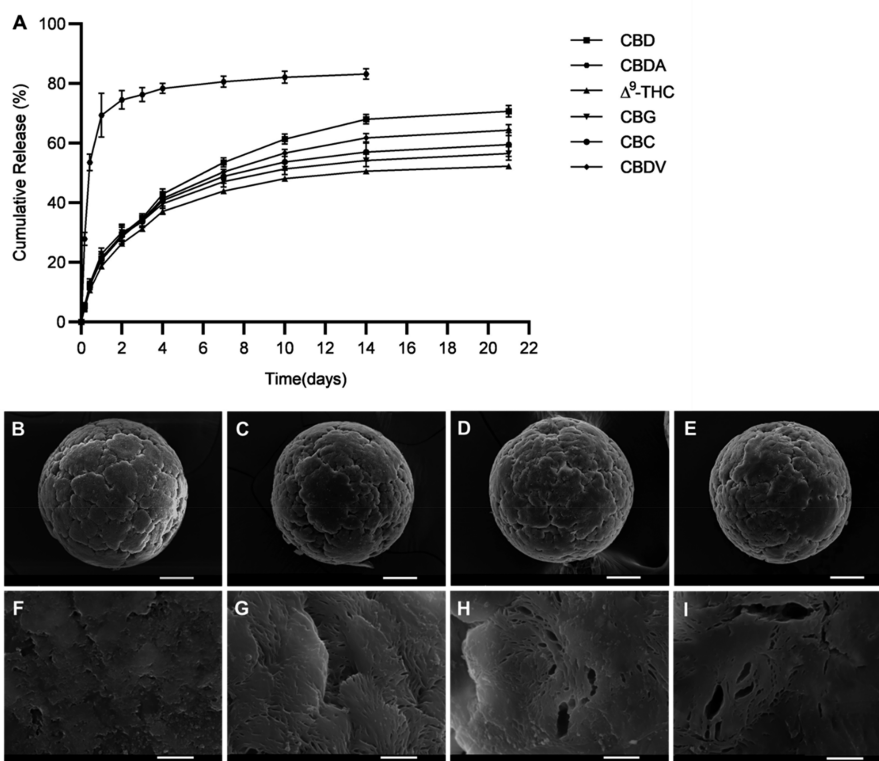

Figure 2. In vitro release study. (A) Phytocannabinoids in vitro release profiles from PCL microdepots loaded with 30 wt % *Cannabis* extract (mean $\pm$ SD, n = 3). (B−I) SEM micrographs depicting the surface morphology of *Cannabis* extract microdepots (B) before and following (C) 7, (D) 14, and (E) 21 days of the in vitro release study. Scale bar: 50 μm. (F−I) Corresponding magnified micrographs of (B−E). Scale bar: 5 μm.
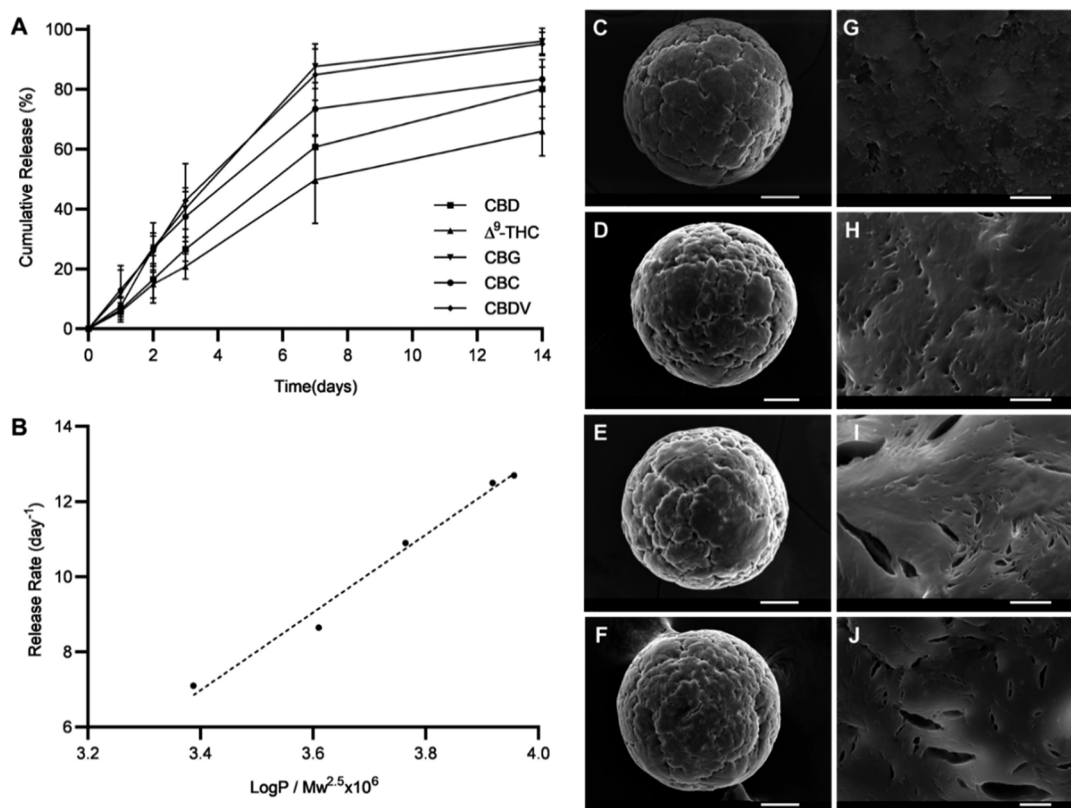
Figure 3. In vivo release study. (A) Phytocannabinoid in vivo release profiles from *Cannabis* extract microdepots recovered from the subcutaneous tissue (mean ± SD, *n* = 4). (B) Average release rate within the first week of the study versus phytocannabinoids' lipophilicity (Log *P*) and molecular weight. The dotted line represents linear regression. (C−J) SEM micrographs depicting the surface morphology of *Cannabis* extract microdepots (C) before and following (D) 3, (E) 7, and (F) 14 days of the in vivo release study. Scale bar: 50 μm. (G−J) Corresponding magnified micrographs of C−F. Scale bar: 5 μm.

molecule propensity for diffusion.[43] The slightly lower cumulative release amounts of CBDV, CBG, Δ^9-THC, and CBC compared to CBD may be related to the lower loadings of these minor phytocannabinoids.[44] The micrographs of the microdepots taken during the dissolution study (Figure 2B−E) revealed no significant changes in microdepot sizes or evidence for surface erosion. Magnified micrographs (Figure 2F−I) show the formation of pores in the microdepots' surface that grew over time from hundreds of nanometers to several micrometers. Pristine PCL microdepots incubated in the same release medium remained intact during the study period, as can be seen in Figure S3. These findings, along with PCL's inherent semicrystalline, low vitreous transition temperature, and hydrophobic nature, suggest that diffusion is the governing mechanism of the *Cannabis* components' release from the polymeric carrier.[27,45,46]

3.3. In Vivo Phytocannabinoid Release.
Biodegradable polymeric microdepots are widely used to deliver medications in a rate-controlled manner.[47] However, direct analysis of these systems during release studies in vivo is rarely reported. The performance of the formulation within the subcutaneous tissue is usually predicted based on in vitro dissolution tests followed by deconvolution of pharmacokinetic data to estimate the in vivo absorption profile.[48,49] These predictions are rarely accurate, because current in vitro environments do not accurately reflect the biological factors present in the subcutaneous environment, that largely affect the drug release kinetics.[50−52] Therefore, to evaluate the in vivo performance of

the formulation, mice were injected with a single subcutaneous injection of *Cannabis*-loaded microdepots, or a *Cannabis* extract solution at an equivalent dose. At different time points, microdepots were collected from the subcutaneous tissue in order to evaluate the amounts of phytocannabinoids released, and phytocannabinoids' serum levels were analyzed to obtain pharmacokinetic profiles.

Because the microdepots did not migrate from the injection site, we were able to recover them (Figure S4) and directly analyze the release behavior in vivo. Phytocannabinoid release profiles were determined according to their remaining content in the retrieved microdepots. CBDA was not detectable in the recovered microdepots 24 h post administration, in correlation with its fast release in vitro. Figure 3A demonstrates sustained phytocannabinoid delivery, with close to zero-order release kinetics during the first week (R^2 > 0.980 in linear regression), followed by a slower release rate during the second week, corresponding to the deceleration in the release rate in vitro after the first week. An empirical model correlating between the phytocannabinoids in vivo release rate within the first week (zero order release rate) and their physiochemical characteristics was examined. As can be seen in Figure 3B, a linear relationship (correlation coefficient of 0.985) between phytocannabinoids' average release rate, lipophilicity (Log *P*) and molecular weight (Mw) was found, following the expression:

$$\text{release rate} \propto \log P/Mw^{2.5}$$

Log P values (logarithm of partition coefficient) were calculated using ChemAxon software. The model depicts that the greater the lipophilicity of a phytocannabinoid, the faster it releases, possibly because of the lipophilic nature of the subcutaneous site. In contrast, the larger the molecules are, the slower they diffuse. This relationship may then be applied to predict the in vivo release behavior of other phytocannabinoids, which might be included in other *Cannabis* strains.

The microstructure of the recovered microdepots was also investigated at different stages of the release study and no signs of surface erosion or deformation were observed (Figure 3C−F). The pores that were formed on the microdepots' surface reached dimensions of several microns after 1 week (Figure 3G−J), faster than in the dissolution study, corroborating with the observed higher released amounts (Figure 3A). In addition, the appearance of the microdepots was documented during the in vitro and in vivo release studies. As shown in Figure 4, the
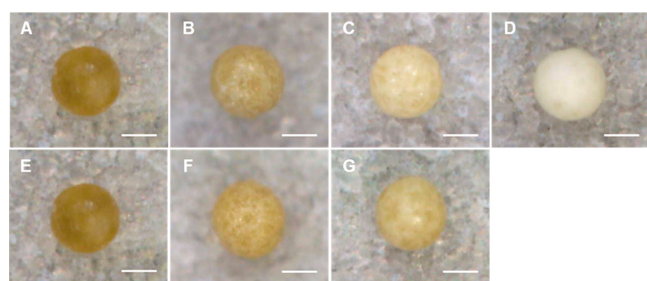

Figure 4. Optical images of *Cannabis* extract microdepots (A) before and following (B) 7, (C) 14, and (D) 21 days of the in vitro release study; and (E) before and following (F) 7 and (G) 14 days of the in vivo release study. Scale bar: 100 μm.

microdepots gradually lost their brown color with time. This might be the result of sustained release from the polymer matrix of other pigment molecules usually present in *Cannabis* extracts, such as flavonoids, carotenoids, and chlorophylls.[7]

Serum levels of 3 predominant neutral phytocannabinoids, CBD, Δ^9-THC, and CBG were measured, and their pharmacokinetic profiles are shown in Figure 5. Because the first blood samples were taken 24 h postdose, phytocannabinoid levels at shorter times were not available. Administration of *Cannabis* extract solution for immediate release resulted in a more abrupt increase in phytocannabinoid bloodstream levels and faster elimination compared to microdepots administration. Importantly, microdepot administration resulted in sustained, elevated serum phytocannabinoid levels, over the 14 day study period. The serum concentration of CBD reached a maximum during the first day following injection, then decreased gradually and was maintained at a steady level, significantly higher than the immediate-release group ($p < 0.05$). To determine the relative bioavailability, we compared the AUC_{1-14} from microdepot administration to the AUC_{1-14} from solution administration of *Cannabis* extract. Over the 14 day time period, the relative bioavailability of the CBD released from the extract in microdepots was more than two-fold higher than that of the extract solution. Significantly higher steady serum levels ($p < 0.05$), enhanced bioavailability and extended absorption duration were observed also for CBG and Δ^9-THC, despite their much lower content. This demonstrates the potential of the formulation to improve the systemic exposure of both major and minor components, which is important for supporting potentially synergistic effects. It should be noted that the microdepots and the immediate-release extract were suspended in the same injection medium for administration, in
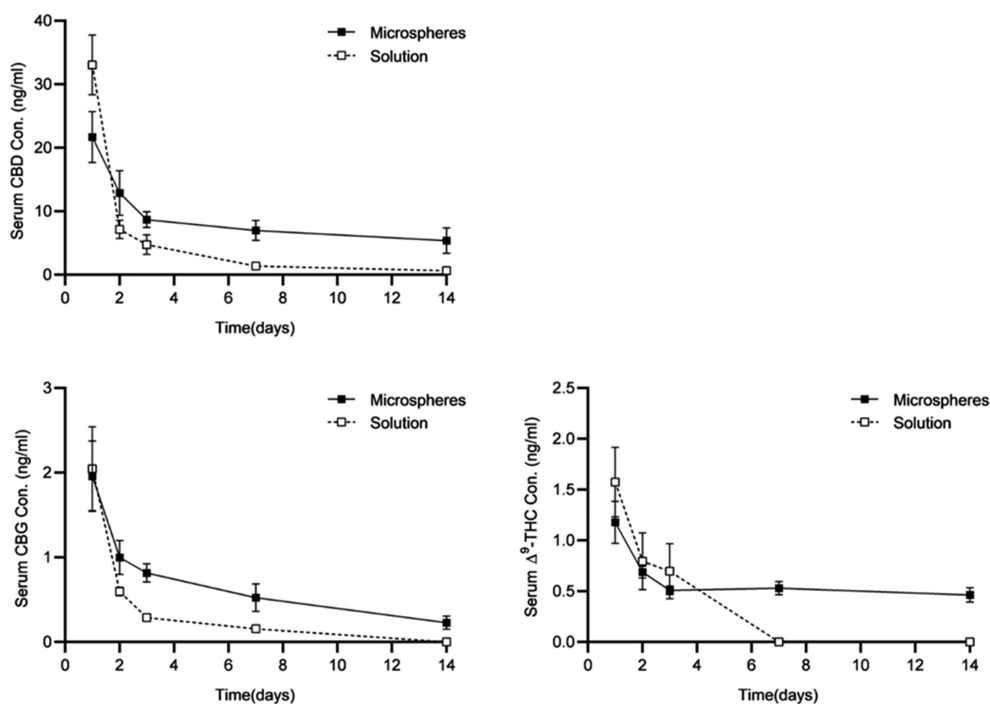

Figure 5. Serum concentration−time profiles of CBD, CBG, and Δ^9-THC following subcutaneous administration of PCL microdepots loaded with 30 wt % *Cannabis* extract (solid line) and *Cannabis* extract solution (dashed line) in mice (mean ± SD, $n = 4$).

order to control for the effects of the medium on the delivery of the therapeutic agents into the bloodstream.

3.4. Microdepot Anticonvulsant Activity. The therapeutic potential of the microdepots as a controlled release formulation for whole-plant *Cannabis* extracts was evaluated via a PTZ model in mice. The specific *Cannabis* extract used was chosen after it has previously demonstrated superior anticonvulsant effects when compared to different equally high-CBD *Cannabis* strains against PTZ-induced convulsions, 30 min post *Cannabis* injections, when phytocannabinoid circulation levels were high.[5] Here, in order to evaluate the long-term activity of the microdepots, we administered PTZ injections to mice 1 week after a single subcutaneous injection of *Cannabis*-loaded microdepots or *Cannabis* extract solution. Mice were monitored for 30 min after induction, and the epileptic seizures were analyzed and ranked according to a seizure profile. The microdepots showed greater reduction in the incidence of tonic-clonic seizures, higher survival rates and increased latency to first tonic-clonic seizure, compared to the extract solution injected control group (Figure 6A, B). In

A

	Solution	Microspheres	p-value
% Mice developing tonic-clonic	100	60	0.02
% Survival	60	90	0.12

Figure 6. Effect of *Cannabis*-loaded microdepots or *Cannabis* extract solution on PTZ-induced convulsions in mice. (A) Incidence of tonic-clonic seizures and percent of mortality protection (compared among groups using the $\chi 2$ test, $p > 0.05$). (B) Latency to first tonic-clonic seizures (mean ± SEM, $*p < 0.05$). (C) CBD, CBG, and Δ^9-THC serum levels 7 days following administration of *Cannabis*-loaded microdepots and pure *Cannabis* extract (mean ± SD).

addition, the phytocannabinoid levels measured at day 7 (Figure 6C) were similar to those obtained in the in vivo release study at the same time point, indicating the reproducible release of the active agents from the polymeric microdepots.

4. DISCUSSION

In this study, we have proposed a novel *Cannabis* delivery system, in the form of polymeric microdepots, for full-spectrum *Cannabis* administration. Encapsulating *Cannabis* extract in a PCL matrix via a one-step printing process was effective in entrapping a wide range of phytocannabinoids in a single polymeric microdepots and modulating their release rate. Similar sustained release of both major and minor phytocannabinoid components was observed and this important for supporting potential synergistic effects of multiple components. Cumulatively higher phytocannabinoid amounts were released from the microdepots in vivo by day 14 and with greater variance between the different phytocanna-

binoids, compared to the in vitro release study. Although only limited information is currently available regarding the in vivo release of pharmaceuticals from PCL, it can be assumed that the faster release kinetics in vivo are a result of an accelerated diffusion rate due to the presence of biological compounds such as lipids.[53,54] These biological factors, which are not accurately represented in vitro, probably contributed to the observed difference in phytocannabinoids' transport rate at the subcutaneous site, as had been shown in the empirical model. This model provided insights into the release and delivery kinetics of several active ingredients in vivo as a function of their physiochemical properties. These findings may contribute to the future development of "polypills" in which multiple active pharmaceutical ingredients are incorporated in a single dosage form.[55] The sustained release enhanced the bioavailability and elevated phytocannabinoid levels in the serum up to 14 days following administration, significantly increasing the in vivo residence time of these highly lipophilic molecules. Moreover, the growing evidence for high-CBD extract's efficacy in treating seizure disorders[14,56] had led us to evaluate the potential of the depots to promote long-term anticonvulsive activity using the PTZ seizure model. PTZ has been previously shown to be a useful model for evaluating cannabinoids anticonvulsant effects in murines.[57−59] The depot's effectiveness against PTZ-induced convulsions was demonstrated 1 week after subcutaneous administration, compared to a bolus of pure *Cannabis* extract. This implies that long-acting microdepots are suitable for the parenteral delivery of medicinal *Cannabis* and might prolong its therapeutic action while attenuating peak serum levels, significantly differing from the current conventional *Cannabis* treatment for epilepsy, based on a twice daily oral dose administration.[60,61] Such systems may provide a convenient and stable long-term treatment for patients suffering from chronic conditions or may supply an alternative delivery form for those incapable of inhaling or swallowing.
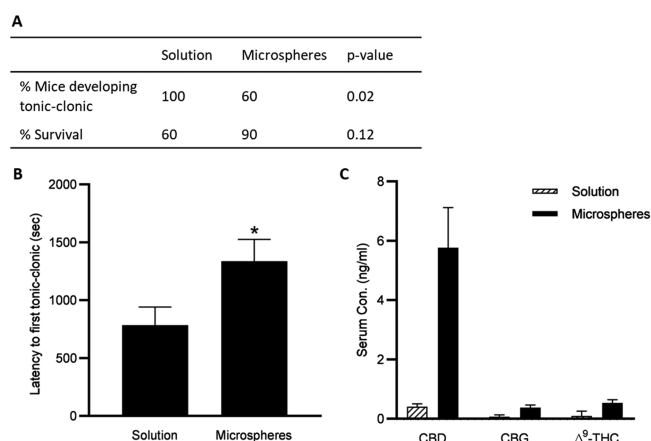
5. CONCLUSIONS

Existing implantable drug delivery depots are designed to release only a single phytocannabinoid, even though it is suggested that whole-plant *Cannabis* extracts have superior therapeutic effects over individual components. Herein, we propose the use of long-acting polymeric microspheres, performing as depots, for the encapsulation and controlled delivery of the full *Cannabis* plant spectrum. In mouse models, we demonstrate that these depots are capable of simultaneously delivering multiple phytocannabinoids and significantly extending their circulation time. Therefore, these depots may be advantageous for harnessing long-term *Cannabis* therapeutic potential while supporting potential synergistic interactions between the plant's components, as demonstrated in an acute convulsion model.

■ ASSOCIATED CONTENT

ⓢ Supporting Information

The Supporting Information is available free of charge at https://pubs.acs.org/doi/10.1021/acsami.0c04435.

> Phytocannabinoid analysis method 1, phytocannabinoid analysis method 2, particle size analysis of *Cannabis* extract microdepots, effect of printing temperature on phytocannabinoids content in the polymer matrix, SEM

micrographs of blank PCL microdepots, *Cannabis* extract microdepot removal from mice (PDF)

Video S1, formation of a *Cannabis*-loaded microdepot upon interaction of the molten jet with the nonwetting surface (MP4)

■ AUTHOR INFORMATION

Corresponding Authors

David Meiri − *The Laboratory of Cancer Biology and Cannabinoid Research, Department of Biology, Technion-Israel Institute of Technology, Haifa 320003, Israel*; Email: dmeiri@technion.ac.il

Dan Y. Lewitus − *Department of Polymers and Plastics Engineering, Shenkar College of Engineering, Design and Art, Ramat-Gan 52526, Israel*; ⓘ orcid.org/0000-0002-6794-7413; Email: lewitus@shenkar.ac.il

Authors

Almog Uziel − *Department of Polymers and Plastics Engineering, Shenkar College of Engineering, Design and Art, Ramat-Gan 52526, Israel*

Anat Gelfand − *The Laboratory of Cancer Biology and Cannabinoid Research, Department of Biology, Technion-Israel Institute of Technology, Haifa 320003, Israel*

Keren Amsalem − *The Laboratory of Cancer Biology and Cannabinoid Research, Department of Biology, Technion-Israel Institute of Technology, Haifa 320003, Israel*

Paula Berman − *The Laboratory of Cancer Biology and Cannabinoid Research, Department of Biology, Technion-Israel Institute of Technology, Haifa 320003, Israel*; ⓘ orcid.org/0000-0002-6821-3307

Gil M. Lewitus − *The Laboratory of Cancer Biology and Cannabinoid Research, Department of Biology, Technion-Israel Institute of Technology, Haifa 320003, Israel*

Complete contact information is available at:
https://pubs.acs.org/10.1021/acsami.0c04435

Notes

The authors declare no competing financial interest.

■ REFERENCES

(1) Ramirez, M. R. Potential Health Benefits of Cannabis Extracts : A Review. *Int. J. Chem. Biomed. Sci.* **2016**, *2* (1), 1−8.

(2) Lata, H.; Chandra, S.; Khan, I. A.; Elsohly, M. A. Propagation through Alginate Encapsulation of Axillary Buds of Cannabis Sativa L. − an Important Medicinal Plant. *Physiol. Mol. Biol. Plants* **2009**, *15* (1), 79−86.

(3) Russo, E. B. Beyond Cannabis : Plants and the Endocannabinoid System. *Trends Pharmacol. Sci.* **2016**, *37* (7), 594−605.

(4) Nallathambi, R.; Mazuz, M.; Namdar, D.; Shik, M.; Namintzer, D.; Vinayaka, A. C.; Ion, A.; Faigenboim, A.; Nasser, A.; Laish, I.; Konikoff, F. M.; Koltai, H. Identification of Synergistic Interaction Between Cannabis-Derived Compounds for Cytotoxic Activity in Colorectal Cancer Cell Lines and Colon Polyps That Induces Apoptosis-Related Cell Death and Distinct Gene Expression. *Cannabis Cannabinoid Res.* **2018**, *3*, 120−135.

(5) Berman, P.; Futoran, K.; Lewitus, G. M.; Mukha, D.; Benami, M.; Shlomi, T.; Meiri, D. A New ESI-LC/MS Approach for Comprehensive Metabolic Profiling of Phytocannabinoids in Cannabis. *Sci. Rep.* **2018**, *8*, DOI: 10.1038/s41598-018-32651-4

(6) Andre, C. M.; Hausman, J.-F.; Guerriero, G. Cannabis Sativa: The Plant of the Thousand and One Molecules. *Front. Plant Sci.* **2016**, *7* (19), DOI: 10.3389/fpls.2016.00019

(7) Brenneisen, R. Chemistry and Analysis of Phytocannabinoids and Other Cannabis Constituents. In *Marijuana and the Cannabinoids*; ElSohly, M. A., Ed.; Humana Press, 2007; pp 17−49.

(8) Gill, E. W.; Paton, W. D. M.; Pertwee, R. G. Preliminary Experiments on the Chemistry and Pharmacology of Cannabis. *Nature* **1970**, *228*, 134−136.

(9) McPartland, J. M.; Russo, E. B. Cannabis and Cannabis Extracts: Greater Than the Sum of Their Parts? *J. Cannabis Ther.* **2001**, *1* (3−4), 103−132.

(10) Bruni, N.; Della Pepa, C.; Oliaro-Bosso, S.; Pessione, E.; Gastaldi, D.; Dosio, F. Cannabinoid Delivery Systems for Pain and Inflammation Treatment. *Molecules* **2018**, *23* (10), 2478.

(11) Russo, E. B. Taming THC: Potential Cannabis Synergy and Phytocannabinoid-Terpenoid Entourage Effects. *Br. J. Pharmacol.* **2011**, *163* (1), 1344−1364.

(12) Maccallum, C. A.; Russo, E. B. Practical Considerations in Medical Cannabis Administration and Dosing. *Eur. J. Intern. Med.* **2018**, *49*, 12−19.

(13) Gallily, R.; Yekhtin, Z.; Hanuš, L. O. Overcoming the Bell-Shaped Dose-Response of Cannabidiol by Using Cannabis Extract Enriched in Cannabidiol. *Pharmacol. Pharm.* **2015**, *6* (2), 75−85.

(14) Pamplona, F. A.; da Silva, L. R.; Coan, A. C. Potential Clinical Benefits of CBD-Rich Cannabis Extracts Over Purified CBD in Treatment-Resistant Epilepsy : Observational Data Meta-Analysis. *Front. Neurol.* **2018**, *9*, 1−9.

(15) Pertwee, R. *Handbook of Cannabis*; Pertwee, R. G., Ed.; Oxford University Press, 2014.

(16) Wagner, H.; Ulrich-Merzenich, G. Synergy Research:Approaching a New Generation of Phytopharmaceuticals. Review (Part 1). *Phytomedicine* **2009**, *16*, 97−110.

(17) Bar-Lev Schleider, L.; Abuhasira, R.; Novack, V. Medical Cannabis: Aligning Use to Evidence-Based Medicine Approach. *Br. J. Clin. Pharmacol.* **2018**, *84* (11), 2458−2462.

(18) Bridgeman, M. B.; Abazia, D. T. Medicinal Cannabis : History, Pharmacology, And Implications for the Acute Care Setting. *P.T.* **2017**, *42* (3), 180−188.

(19) Hazekamp, A.; Ware, M. A.; Muller-Vahl, K. R.; Abrams, D.; Grotenhermen, F. The Medicinal Use of Cannabis and Cannabinoids-An International Cross-Sectional Survey on Administration Forms. *J. Psychoact. Drugs* **2013**, *45* (3), 199−210.

(20) Huynh, C. T.; Lee, D. S. Controlled Release. In *Encyclopedia of Polymeric Nanomaterials*; Kobayashi, S., Müllen, K., Eds.; Springer, 2014.

(21) Karschner, E. L.; Darwin, W. D.; Goodwin, R. S.; Wright, S.; Huestis, M. A. Plasma Cannabinoid Pharmacokinetics Following Controlled Oral Δ(9)-Tetrahydrocannabinol and Oromucosal Cannabis Extract Administration. *Clin. Chem.* **2011**, *57* (1), 66−75.

(22) Duran-Lobato, M.; Munoz-Rubio, I.; Holgado, M. A.; Alvarez-Fuentes, J.; Fernandez-Arevalo, M.; Martin-Banderas, L. Enhanced Cellular Uptake and Biodistribution of a Synthetic Cannabinoid Loaded in Surface-Modified Poly(Lactic-Co-Glycolic Acid) Nanoparticles. *J. Biomed. Nanotechnol.* **2014**, *10* (6), 1068−1079.

(23) Paolino, D.; Cosco, D.; Cilurzo, F.; Fresta, M. Innovative Drug Delivery Systems for the Administration of Natural Compounds. *Curr. Bioact. Compd.* **2007**, *3* (4), 262−277.

(24) Teekamp, N.; Van Dijk, F.; Broesder, A.; Evers, M.; Zuidema, J.; Steendam, R.; Post, E.; Hillebrands, J.L.; Frijlink, H.W.; Poelstra, K. Polymeric Microspheres for the Sustained Release of a Protein-Based

Drug Carrier Targeting the PDGF β -Receptor in the Fi Brotic Kidney. *Int. J. Pharm.* **2017**, *534* (1−2), 229−236.

(25) Yang, F.; Niu, X.; Gu, X.; Xu, C.; Wang, W.; Fan, Y. Biodegradable Magnesium-Incorporated Poly(l-Lactic Acid) Microspheres for Manipulation of Drug Release and Alleviation of Inflammatory Response. *ACS Appl. Mater. Interfaces* **2019**, *11* (26), 23546−23557.

(26) Martín Banderas, L.; Álvarez Fuentes, J.; Durán Lobato, M.; Prados, J.; Melguizo, C.; Fernández Arévalo, M.; Holgado, M. Á. Cannabinoid Derivate Loaded PLGA Nanocarriers for Oral Administration: Formulation, Characterization, and Cytotoxicity. *Int. J. Nanomed.* **2012**, *7*, 5793−5806.

(27) Hernan Perez de la Ossa, D.; Ligresti, A.; Gil-Alegre, M.E.; Aberturas, M.R.; Molpeceres, J.; Di Marzo, V.; Torres Suarez, A.I. Poly-ε-Caprolactone Microspheres as a Drug Delivery System for Cannabinoid Administration: Development, Characterization and in Vitro Evaluation of Their Antitumoral Efficacy. *J. Controlled Release* **2012**, *161* (3), 927−932.

(28) De La Ossa, D. H. P.; Gil-Alegre, M. E.; Ligresti, A.; Aberturas, M. D. R.; Molpeceres, J.; Torres, A. I.; Di Marzo, V. Preparation and Characterization of Δ9- Tetrahydrocannabinol-Loaded Biodegradable Polymeric Microparticles and Their Antitumoral Efficacy on Cancer Cell Lines. *J. Drug Target.* **2013**, *21* (8), 710−718.

(29) Martín-Banderas, L.; Muñoz-Rubio, I.; Prados, J.; Álvarez-Fuentes, J.; Calderón-Montaño, J. M.; López-Lázaro, M.; Arias, J. L.; Leiva, M. C.; Holgado, M. A.; Fernández-Arévalo, M. In Vitro and in Vivo Evaluation of Δ9-Tetrahidrocannabinol/PLGA Nanoparticles for Cancer Chemotherapy. *Int. J. Pharm.* **2015**, *487* (1−2), 205−212.

(30) Berrocoso, E.; Rey-Brea, R.; Fernández-Arévalo, M.; Micó, J. A.; Martín-Banderas, L. Single Oral Dose of Cannabinoid Derivate Loaded PLGA Nanocarriers Relieves Neuropathic Pain for Eleven Days. *Nanomedicine* **2017**, *13*, 2623−2632.

(31) Hernan Perez de la Ossa, D.; Lorente, M.; Gil-Alegre, M. E.; Torres, S.; Garcia-Taboada, E.; Aberturas, M. d. R.; Molpeceres, J.; Velasco, G.; Torres-Suarez, A. I. Local Delivery of Cannabinoid-Loaded Microparticles Inhibits Tumor Growth in a Murine Xenograft Model of Glioblastoma Multiforme. *PLoS One* **2013**, *8* (1), e54795.

(32) Kamali, A.; Oryan, A.; Hosseini, S.; Ghanian, M. H.; Alizadeh, M.; Baghaban Eslaminejad, M.; Baharvand, H. Cannabidiol-Loaded Microspheres Incorporated into Osteoconductive Scaffold Enhance Mesenchymal Stem Cell Recruitment and Regeneration of Critical-Sized Bone Defects. *Mater. Sci. Eng., C* **2019**, *101* (March), 64−75.

(33) Shpigel, T.; Uziel, A.; Lewitus, D. Y. SPHRINT − Printing Drug Delivery Microspheres from Polymeric Melts. *Eur. J. Pharm. Biopharm.* **2018**, *127*, 398−406.

(34) Arica, B.; Kaş, H. S.; Moghdam, A.; Akalan, N.; Hincal, A. A. Carbidopa/Levodopa-Loaded Biodegradable Microspheres: In Vivo Evaluation on Experimental Parkinsonism in Rats. *J. Controlled Release* **2005**, *102* (3), 689−697.

(35) Shpigel, T.; Cohen Taguri, G.; Lewitus, D. Y. Controlling Drug Delivery from Polymer Microspheres by Exploiting the Complex Interrelationship of Excipient and Drug Crystallization. *J. Appl. Polym. Sci.* **2019**, *136* (6), 47227.

(36) Durán-Lobato, M.; Martín-Banderas, L.; Gonçalves, L. M. D.; Fernández-Arévalo, M.; Almeida, A. J. Comparative Study of Chitosan- and PEG-Coated Lipid and PLGA Nanoparticles as Oral Delivery Systems for Cannabinoids. *J. Nanopart. Res.* **2015**, *17*, 61.

(37) Jyothi, N. V. N.; Prasanna, P. M.; Sakarkar, S. N.; Prabha, K. S.; Ramaiah, P. S.; Srawan, G. Y. Microencapsulation Techniques, Factors Influencing Encapsulation Efficiency. *J. Microencapsulation* **2010**, *27* (3), 187−197.

(38) Kollamaram, G.; Croker, D. M.; Walker, G. M.; Goyanes, A.; Basit, A. W.; Gaisford, S. Low Temperature Fused Deposition Modeling (FDM) 3D Printing of Thermolabile Drugs. *Int. J. Pharm.* **2018**, *545* (1−2), 144−152.

(39) Huang, S.; O'Donnell, K. P.; Delpon de Vaux, S. M.; O'Brien, J.; Stutzman, J.; Williams, R. O. Processing Thermally Labile Drugs by Hot-Melt Extrusion: The Lesson with Gliclazide. *Eur. J. Pharm. Biopharm.* **2017**, *119*, 56−67.

(40) Thomas, B. F.; ElSohly, M. A. *The Analytical Chemistry of Cannabis Emerging Issues in Analytical Chemistry*; Elsevier, 2016.

(41) Trofin, I. G.; Dabija, G.; Vaireanu, D. I.; Filipescu, L. Long-Term Storage and Cannabis Oil Stability. *Rev. Chim. -Bucharest* **2012**, *53*, 293−296.

(42) Carbone, M.; Castelluccio, F.; Daniele, A.; Sutton, A.; Ligresti, A.; Di Marzo, V.; Gavagnin, M. Chemical Characterisation of Oxidative Degradation Products of Δ9-THC. *Tetrahedron* **2010**, *66* (49), 9497−9501.

(43) Tuovinen, L.; Peltonen, S.; Jarvinen, K. Drug Release from Starch-Acetate Films. *J. Controlled Release* **2003**, *91*, 345−354.

(44) Aydin, O.; Aydin, B.; Tezcaner, A.; Keskin, D. Study on Physiochemical Structure and in Vitro Release Behaviors of Doxycycline-Loaded PCL Microspheres. *J. Appl. Polym. Sci.* **2015**, *132*, 1−13.

(45) Seyednejad, H.; Gawlitta, D.; Kuiper, R. V.; de Bruin, A.; van Nostrum, C. F.; Vermonden, T.; Dhert, W. J.A.; Hennink, W. E. Biomaterials In Vivo Biocompatibility and Biodegradation of 3D-Printed Porous Scaffolds Based on a Hydroxyl-Functionalized Poly (ε -Caprolactone). *Biomaterials* **2012**, *33* (17), 4309−4318.

(46) Pohlmann, A. R.; Fonseca, F. N.; Paese, K.; Detoni, C. B.; Coradini, K.; Beck, R. C. R.; Guterres, S. S. Poly (e -Caprolactone) Microcapsules and Nanocapsules in Drug Delivery. *Expert Opin. Drug Delivery* **2013**, *10* (5), 623−638.

(47) Kamaly, N.; Yameen, B.; Wu, J.; Farokhzad, O. C. Degradable Controlled-Release Polymers and Polymeric Nanoparticles : Mechanisms of Controlling Drug Release. *Chem. Rev.* **2016**, *116* (4), 2602−2663.

(48) Doty, A. C.; Weinstein, D. G.; Hirota, K.; Olsen, K. F.; Ackermann, R.; Wang, Y.; Choi, S.; Schwendeman, S. P. Mechanisms of in Vivo Release of Triamcinolone Acetonide from PLGA Microspheres. *J. Controlled Release* **2017**, *256*, 19−25.

(49) Shen, J.; Burgess, D. J. In Vitro-in Vivo Correlation for Complex Non-Oral Drug Products: Where Do We Stand? *J. Controlled Release* **2015**, *219*, 644−651.

(50) van Dijk, F.; Teekamp, N.; Beljaars, L.; Post, E.; Zuidema, J.; Steendam, R.; Kim, Y.O.; Frijlink, H.W.; Schuppan, D.; Poelstra, K.; Hinrichs, W.L.J.; Olinga, P. Pharmacokinetics of a Sustained Release Formulation of PDGFβ-Receptor Directed Carrier Proteins to Target the Fibrotic Liver. *J. Controlled Release* **2018**, *269*, 258−265.

(51) Zolnik, B. S.; Burgess, D. J. Evaluation of in Vivo − in Vitro Release of Dexamethasone from PLGA Microspheres. *J. Controlled Release* **2008**, *127*, 137−145.

(52) Iyer, S. S.; Barr, W. H.; Karnes, H. T. Profiling In Vitro Drug Release from Subcutaneous Implants : A Review of Current Status and Potential Implications on Drug Product Development. *Biopharm. Drug Dispos.* **2006**, *27*, 157−170.

(53) Doty, A. C.; Hirota, K.; Olsen, K. F.; Sakamoto, N.; Ackermann, R.; Feng, M. R.; Wang, Y.; Choi, S.; Qu, W.; Schwendeman, A.; Schwendeman, S. P. Validation of a Cage Implant System for Assessing in Vivo Performance of Long-Acting Release Microspheres. *Biomaterials* **2016**, *109*, 88−96.

(54) Tracy, M. A.; Ward, K. L.; Firouzabadian, L.; Wang, Y.; Dong, N.; Qian, R.; Zhang, Y. Factors Affecting the Degradation Rate of Poly(Lactide-Co-Glycolide) Microspheres in Vivo and in Vitro. *Biomaterials* **1999**, *20*, 1057−1062.

(55) Khaled, S. A.; Burley, J. C.; Alexander, M. R.; Yang, J.; Roberts, C. J. 3D Printing of Five-in-One Dose Combination Polypill with Defined Immediate and Sustained Release Profiles. *J. Controlled Release* **2015**, *217*, 308−314.

(56) Kaplan, J. S.; Stella, N.; Catterall, W. A.; Westenbroek, R. E. Cannabidiol Attenuates Seizures and Social Deficits in a Mouse Model of Dravet Syndrome. *Proc. Natl. Acad. Sci. U. S. A.* **2017**, *114* (42), 11229−11234.

(57) Hill, T. D. M.; Cascio, M. G.; Romano, B.; Duncan, M.; Pertwee, R. G.; Williams, C. M.; Whalley, B. J.; Hill, A. J. Cannabidivarin-Rich Cannabis Extracts Are Anticonvulsant in Mouse and Rat via a CB1 Receptor-Independent Mechanism. *Br. J. Pharmacol.* **2013**, *170* (3), 679−692.

(58) Jones, N. A.; Hill, A. J.; Smith, I.; Bevan, S. A.; Williams, C. M.; Whalley, B. J.; Stephens, G. J. Cannabidiol Displays Antiepileptiform and Antiseizure Properties in Vitro and in Vivo. *J. Pharmacol. Exp. Ther.* **2010**, *332* (2), 569–577.

(59) Consroe, P.; Benedito, M. A. C.; Leite, J. R.; Carlini, E. A.; Mechoulam, R. Effects of Cannabidiol on Behavioral Seizures Caused by Convulsant Drugs or Current in Mice. *Eur. J. Pharmacol.* **1982**, *83* (3–4), 293–298.

(60) McCoy, B.; Wang, L.; Zak, M.; Al-Mehmadi, S.; Kabir, N.; Alhadid, K.; McDonald, K.; Zhang, G.; Sharma, R.; Whitney, R.; Sinopoli, K.; Snead, O. C. A Prospective Open-Label Trial of a CBD/THC Cannabis Oil in Dravet Syndrome. *Ann. Clin. Transl. Neurol.* **2018**, *5* (9), 1077–1088.

(61) Suraev, A.; Lintzeris, N.; Stuart, J.; Kevin, R. C.; Blackburn, R.; Richards, E.; Arnold, J. C.; Ireland, C.; Todd, L.; Allsop, D. J.; McGregor, I. S. Composition and Use of Cannabis Extracts for Childhood Epilepsy in the Australian Community. *Sci. Rep.* **2018**, *8* (1), 1–14.